

# CFD Study of Flow and Heat Transfer during Compression Process in a Liquid Piston for Isothermal Compressed Air Energy Storage

GOUDA El Mehdi<sup>1</sup>, BENAOUICHA Mustapha<sup>2</sup>, NEU Thibault<sup>2</sup>, FAN Yilin<sup>1</sup>, LUO Lingai<sup>1</sup>

<sup>1</sup>Nantes Université, CNRS, Laboratoire de Thermique et Énergie de Nantes, LTeN, UMR 6607  
F-44000 Nantes, France

[El-mehdi.gouda@univ-nantes.fr](mailto:El-mehdi.gouda@univ-nantes.fr); [Mustapha.BENAOUICHA@segula.fr](mailto:Mustapha.BENAOUICHA@segula.fr); [Thibault.NEU@segula.fr](mailto:Thibault.NEU@segula.fr)

<sup>2</sup>Segula Technologies. Naval and Energy Engineering Research and Innovation Unit.

9 avenue Edouard Belin, 92500 Rueil-Malmaison, France

[Yilin.fan@univ-nantes.fr](mailto:Yilin.fan@univ-nantes.fr); [Lingai.luo@univ-nantes.fr](mailto:Lingai.luo@univ-nantes.fr)

**Abstract** - Liquid piston technology has proved its efficiency into the achievement of Isothermal Compressed Air Energy Storage. While the concept is no more a new one, the description and the understanding of the physics of the flow and heat transfer during compression process are not completely achieved. Through a CFD study based on the resolution of Navier-stokes equations and VOF method for interface tracking, a characterization of the flow and heat transfer inside the liquid piston, which are complex, are presented. The numerical results were validated and compared with the ones obtained in a former experimental study. Both velocity and temperature fields and profiles are analyzed locally and globally. In this study, it is found that with a compression ratio of 5 and compression time of 21s, the air's average temperature rises non linearly with 32K. The velocity and temperature profiles undergo several stages. A characteristic structure appears at the beginning of the compression where the flow is axisymmetric and remains so until its disruption. It is observed that the structure disruption occurs closer to the cylinder head moments after the highest local velocities are observed. Velocity fields analysis show that the air's velocity can be higher than 10 time the piston velocity.

**Keywords:** Compressed air energy storage (CAES); Liquid Piston (LP); Air compression; Flow regime; VOF method; Heat transfer

## 1. Introduction

New generations of CAES (Compressed Air Energy Storage) systems such as REMORA [1] and GLIDES [2] lean towards Isothermal compression/expansion. To achieve this type of processes the liquid piston concept has been proposed. It improved the efficiency of compressed air storage systems by allowing near-isothermal compression to be achieved [3], [4]. This process is ensured by maximizing heat exchanges between the compressed gas and its environment, making it possible to minimize the work provided by the piston. These heat exchanges are favored by the low forward velocity of the liquid column and the large gas/wall exchange surface [3]. This exchange surface is significantly greater than that of conventional pistons since the compression chamber allows a higher Length/Diameter ratio  $\frac{L}{D} \gg 1$ ). In addition, the liquid piston eliminates the leakage and friction problems associated with sealing and machining the cylinder and piston [5].

Van De Ven and Li obtained 19% decrease in energy consumption by the liquid piston compared to the conventional piston, as well as a 13% increase in efficiency [3], showing the interest development of this technology. Subsequently, many numerical and experimental works were carried out to better characterize the compression/expansion processes using a liquid piston [2], [5], [6]. They mainly focused on the global aspects (air's temperature and pressure) of the processes and heat transfer, while the evolution of the flow inside the liquid piston is still uncharacterized. Recently, through Particle Image Velocimetry (PIV) experiments, Neu and Subrenat showed that the flow undergoes several stages [7]. The present numerical study investigates the flow and heat transfer inside a liquid piston during a compression process. The results are compared to those obtained experimentally for Neu's and Subrenat's study [7].

The paper is organized as follows. Firstly, the numerical model is presented. Then the geometry and numerical parameters are listed. The evolution low and heat transfer is described and comparison results are performed. Finally, key findings of the study are noted in a conclusion.

## 2. Numerical model

The mathematical model of the multiphase flow and the VOF method used in the study are briefly presented in this section. In order to define a two-phase problem, the volume fraction  $\alpha$  is defined in Eq (1):

$$\alpha = \frac{V_{water}}{V_{cell}} \quad (1)$$

Where  $V_{water}$  is the control volume of water inside a mesh cell  $V_{cell}$ .

The Navier-Stokes system for the compressible multiphase flow is given by :

$$\frac{\partial \rho}{\partial t} + \nabla \cdot (\rho \mathbf{U}) = 0 \quad (2)$$

$$\frac{\partial \rho \mathbf{U}}{\partial t} + \nabla \cdot (\rho \mathbf{U} \mathbf{U}) - \nabla \cdot (\mu \nabla \mathbf{U}) = \sigma \kappa \nabla \alpha - \mathbf{g} \cdot \mathbf{x} \nabla \rho - \nabla P' \quad (3)$$

$$\frac{\partial \rho T}{\partial t} + \nabla \cdot (\rho \mathbf{U} T) - \nabla \cdot (\mu T) = - \left( \frac{\alpha}{c_{v, eau}} + \frac{1 - \alpha}{c_{v, air}} \right) \left( \frac{\partial \rho e_k}{\partial t} + \nabla \cdot (\rho \mathbf{U} e_c) + \nabla \cdot (\mathbf{U} P) \right) \quad (4)$$

Where  $\mathbf{U}$  represents the velocity vector,  $\sigma$  is the surface tension coefficient,  $\kappa$  is the curvature of the interface is calculated as  $\kappa = \nabla \cdot \left( \frac{\nabla \alpha}{|\nabla \alpha|} \right)$ .  $P' = P - \rho \mathbf{g} \cdot \mathbf{x}$  is the dynamic pressure,  $\mathbf{g}$  is the gravitational acceleration and  $\mathbf{x}$  is the position vector.

$e_k = \frac{|\mathbf{U}|^2}{2}$  is the specific kinetic energy,  $c_{v, water}$  and  $c_{v, air}$  are the specific heat capacities at constant volume for the water and air phases, respectively.

Eq. 5 shows the transport equation for the water volume fraction  $\alpha$  used to capture the free surface:

$$\frac{\partial \alpha}{\partial t} + \nabla \cdot (\mathbf{U} \alpha) + \nabla \cdot (\mathbf{U}_r \alpha (1 - \alpha)) = 0 \quad (5)$$

Where  $\nabla \cdot (\mathbf{U}_c \alpha (1 - \alpha))$  is an anti-diffusion term used to make a sharper water/air interface and  $\mathbf{U}_r = \mathbf{U}_{water} - \mathbf{U}_{air}$  is the vector of relative velocity, called as the "compression velocity".

Open-source code OpenFOAM, through CompressibleInterFoam solver is used to implement the above model [7].

Large Eddy Simulation (LES-WALE) model is chosen for turbulence modeling is chosen. It has proven its efficiency for this type of flow [8], [9].

## 3. Numerical And Physical Parameters

To enable experimental comparison and validation of numerical results, the geometry and the parameters of the study are the same ones as those in Neu and Subrenat (Table 1) [7]. The liquid piston is modeled as a 3D cylinder with  $L_{ini}$  length and  $D$  diameter (Figure 1).  $L_{pist}$  is the position of the water/air interface at time  $t$ . The piston walls are considered isothermal at  $T = T_{walls}$  and the domain is at an initial temperature  $T_{ini}$ . The initial domain is only filled with air  $L_{pist} = 0m$  and water is injected from the bottom at a constant speed  $U_{pist} = 0,033 m \cdot s^{-1}$ .

## 4. Results And Discussion

The results obtained numerically (evolution of air's average temperature  $T_{air, ave}$  and the pressure through time) are compared to those obtained experimentally in a previous study [7]. A mesh convergence study is conducted and the chosen mesh is an O-grid with  $9 \times 10^5$  hexahedral cells. During the compression process, water properties remain constant, no significant temperature evolution is observed and water flow has a parabolic profile. The water/air interface remains flat. The main domain of interest is the air's one, where, during the compression process, the air's temperature raises and the flow and heat transfer show different stages (A, B, C and D) (Figure 2).

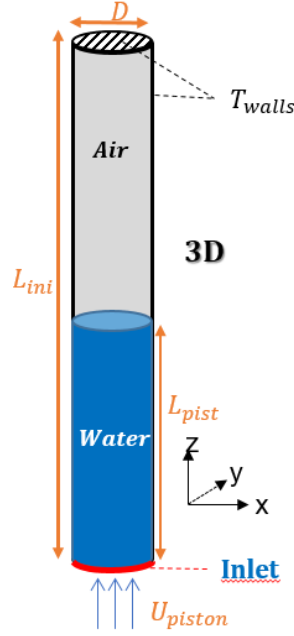


Figure 1: Geometry of the studied configuration (adapted from [10])

Tableau 1 : Physical and numerical parameters of the simulations

Parameter	Value
$T_{walls} (K)$	293
$T_{ini} (K)$	293
$U_{pist} (m \cdot s^{-1})$	0.033
$D (m)$	0.0518
$L_{ini} (m)$	0.906
$P_{ini} (Pa)$	101325
$t_f (s)$	21
$Re_{air}$	104
$Re_{water}$	1706

During the first two stages (A and B) an axisymmetric flow is established where negative velocities (opposite direction to the piston advancement) are observed close the piston walls and positive ones are present in the piston center. These velocities are higher than  $U_{pist}$  and vary from  $-5 \times U_{pist}$  to  $12 \times U_{pist}$ . The evolution of  $T_{air,ave}$  is relatively slow until mid-compression.

At  $t \sim 9.5s$  (Stage C) the curve of  $T_{air,ave}$  is flattened and the flow regime undergoes a transition from a structured one to a chaotic one. The flow is no more axisymmetric after stage B where its structure is disrupted.

During stage D, the evolution of  $T_{air,ave}$  is faster and the flow is totally chaotic and agitated while positive and negative velocities can still be observed.

At the end of the compression  $t = 21s$ , the piston has traveled  $L_{pist} = 0.693m$ , the air's average temperature is  $T_f = 325.4K$ ,  $\Delta T = 32.4K$  and the final pressure  $P_f = 4,8 \times 10^5 Pa = 4.8 \times P_{ini}$ .

Comparison between experimental and numerical results shows the same evolution of  $T_{air,ave}$ . Numerical results remain, during all the compression process inside the experimental error margin measured by Neu and Subrenat at  $\sigma = 2.6K$  [7]. The same stages of flow evolution can be observed, with the flow and heat transfer transition occurring 0.6s later numerically than experimentally (Figure 2).

## 5. Conclusion

This study deals with the numerical modeling of multiphase water/air flow during liquid piston compression for application to compressed air energy storage systems. The numerical results were compared to those obtained experimentally and later validated. Four major stages of the flow have been identified and characterized. An axisymmetric flow is observed until mid-compression when the flow becomes chaotic. A transition of the flow regime is highlighted. It goes from laminar to chaotic and briefly passing through a transient regime. This transition of the flow regime has been observed both numerically and experimentally at  $t \sim 10s$ . At the end of the compression, the final evolution of the air's average temperature is  $\Delta T = 32.4K$  (29.9K experimentally).

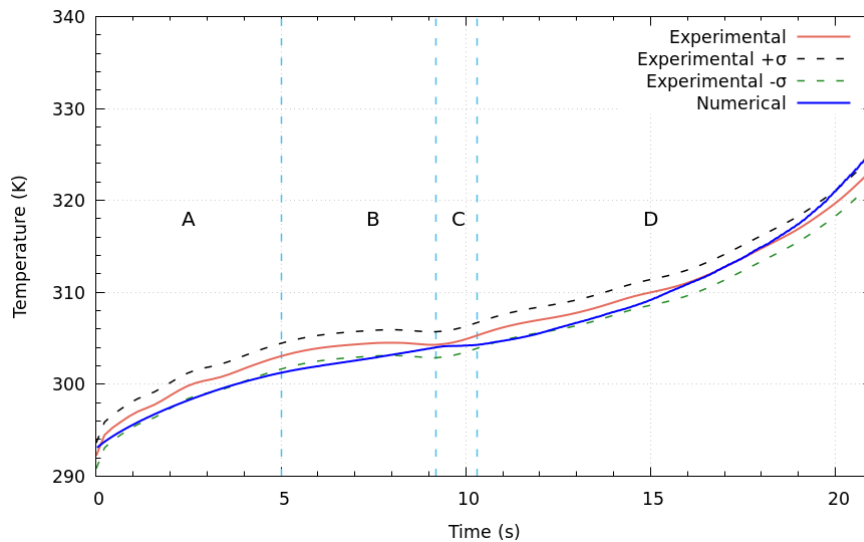


Figure 2: Comparison of the evolution of the average air temperature between the experimental and numerical results.  $\sigma = 2.6K$  is the error margin of the experimental results (adapted from [10])

## Acknowledgements

The present work is supported by CNRS and by France Relance recovery plan of French state of 21 December 2020.

## References

- [1] T. Neu, "Device and method for converting and storing electric energy in the form of compressed air," WO/2016/193322, 08-Dec-2016.
- [2] A. Odukomaiya *et al.*, "Thermal analysis of near-isothermal compressed gas energy storage system," *Appl. Energy*, vol. 179, pp. 948–960, 2016.
- [3] J. D. Van de Ven and P. Y. Li, "Liquid piston gas compression," *Appl. Energy*, vol. 86, no. 10, pp. 2183–2191, Oct. 2009.
- [4] V. C. Patil and P. I. Ro, "Modeling of liquid-piston based design for isothermal ocean compressed air energy storage system," *J. Energy Storage*, vol. 31, p. 101449, Oct. 2020.
- [5] T. Neu, C. Solliec, and B. dos Santos Piccoli, "Experimental study of convective heat transfer during liquid piston compressions applied to near isothermal underwater compressed-air energy storage," *J. Energy Storage*, vol. 32, p. 101827, Dec. 2020.
- [6] V. C. Patil and P. I. Ro, "Experimental study of heat transfer enhancement in liquid piston compressor using aqueous foam," *Appl. Therm. Eng.*, vol. 164, Jan. 2020.
- [7] T. Neu and A. Subrenat, "Experimental investigation of internal air flow during slow piston compression into isothermal compressed air energy storage," *J. Energy Storage*, vol. 38, p. 102532, Jun. 2021.
- [8] E. M. Gouda, M. Benaouicha, T. Neu, L. Luo, and Y. Fan, "Méthode VOF pour la simulation numérique de l'écoulement de l'air comprimé et du transfert thermique associé dans un piston liquide," in *24e Congrès Français de Mécanique (CFM2019)*, 2019, pp. 220–226.
- [9] E. M. Gouda, "Investigation of a compressed air energy storage system : flow and heat transfer numerical modeling in a liquid piston," University of Nantes, 2021.
- [10] E. M. Gouda, M. Benaouicha, T. Neu, Y. Fan, and L. Luo, "Flow and heat transfer characteristics of air compression in a liquid piston for compressed air energy storage," *Energy*, 2022.